



Green Synthesis of Silver Nanoparticles using Egyptian Propolis extract and its Antimicrobial Activity

Samir Osman. Mohamed^{1,2,3}, Karim El-Naggar¹, Mostafa M.H. Khalil^{1*}



¹ Chemistry Department, Faculty of Science, Ain Shams University, Abbassia, 11566, Cairo, Egypt.

² Physics Department, Faculty of Science, Ibb University, Ibb, Yemen

³ Faculty of Engineering, Al-janad University for Science & Technology, Taiz, Yemen

Abstract

There is great research interest in synthesizing nanomaterials using environmentally friendly methods due to the many applications of these materials in several fields. In this paper, a facile and green chemistry method was used to synthesize silver nanoparticles (AgNPs) using the Egyptian propolis as reducing and capping agent. Different parameters such as aqueous propolis extract quantity, pH, reaction time, and temperature were investigated to get the optimal conditions for synthesis of AgNPs. When aqueous silver nitrate solution is mixed with aqueous propolis extract, the silver ions are rapidly reduced, resulting in the production of extremely stable, crystalline silver nanoparticles in solution. The biosynthesized silver nanoparticles were characterized using different techniques (FTIR, XRD, Zeta potential, TEM, SEM, and EDX). The sizes of the as synthesized silver nanoparticles were 9.43 and 11.39 nm, according to TEM and XRD analysis, respectively. A negative Zeta potential of -8.8 mV were obtained suggesting stabilization of the AgNPs colloidal solution. The antimicrobial activity of biosynthesized silver nanoparticles against *Staphylococcus aureus* and *Escherichia coli* was examined and showed a synergism between propolis and AgNPs as expected for gram-negative bacteria *Escherichia coli* while there was no effect for the extract at the concentrations used. The results proved that biosynthesized AgNPs using Egyptian propolis is promising to be an effective antimicrobial product to be used in infections.

Keywords: Biosynthesis; Silver nanoparticles; Propolis extract; antimicrobial; AgNPs.

1. Introduction

Nanomaterials are critical in the development of potential sustainable technology for humankind. The green chemistry method of nanoparticles synthesis by biomaterial substances connects between nanotechnology and biotechnology. This branch of chemistry; green chemistry, uses biomaterial substances for the bio-reduction of metal ions into their elemental form in the size range of 1–100 nm and it is known as green nanoparticle synthesis. Green synthesis is more reliable, faster, and cost-effective, and it can be easily scaled up to handle larger operations [1, 2].

Nanoparticles have major uses in a variety of industrialized goods such as paints, plastics, metals, ceramics, and magnetic articles. A significant part of nanotechnology is the development of nanoparticles with unique properties for different applications.

Physical and chemical approaches are not as pure, nontoxic, or environmentally friendly as biosynthesis of nanoparticles (metal, metal oxides, and metal composites). Instance, one of the aims of green nanoparticle synthesis is to reduce waste and incorporate sustainable processes. To achieve this aim, green processes that use mild reaction conditions and nontoxic precursors have been emphasized in the production of nanomaterials in recent years in order to promote environmental sustainability [1, 3].

Metal-based nanoparticles are now synthesized from a variety of plant components, including leaves, roots, flowers, and seeds, for a variety of applications [4]. For long time and recently, many researches have shown that biological extracts can be used, effectively, as a non-hazardous precursor for the synthesis of nanomaterials. Several nanoparticles,

* Corresponding author: Mostafa M. H. Khalil (khalil62@yahoo.com, mostafa_khalil@sci.asu.edu.eg)

Receive Date: 06 November 2021, **Revise Date:** 07 December 2021, **Accept Date:** 12 December 2021,

First Publish Date: 12 December 2021

DOI: 10.21608/EJCHEM.2021.104296.4838

©2022 National Information and Documentation Center (NIDOC)

such as cobalt, copper, silver, gold, palladium, platinum, zinc oxide, and magnetite, have been successfully synthesized using plants [2, 5, 6].

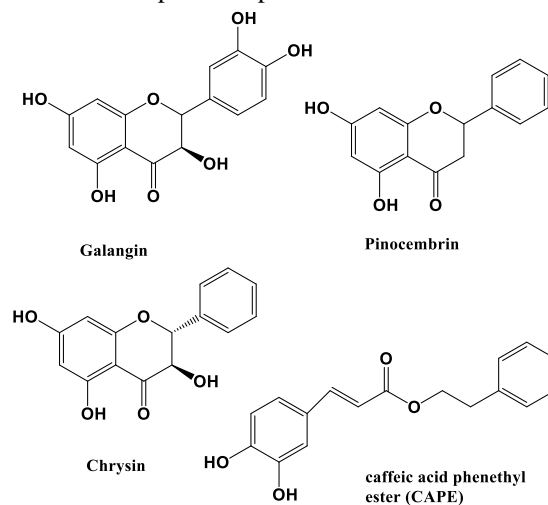
Silver is a lustrous, soft, white element with a high electrical and thermal conductivity that is found in a transition column with Copper and Gold. It was well-known that silver has its medical and therapeutic advantages before the discovery of infectious microbes. Silver is used in a variety of ways, including tokens, solutions, vessels, foil, sutures, and colloids such as lotions, unguents, and so on. Because of their appealing physicochemical properties, silver nanoparticles play an important role in biology and medicine research. Silver contained products have long been known to have significant inhibitory and broad antimicrobial activities. They have been used to prevent and treat a variety of diseases, most notably infections. So, researchers have been paying close attention to synthesis and applications of nano-silver because of their exceptional protection against a wide variety of microorganisms [7–11]. Because of its rapid, eco-friendly, non-pathogenic, economical protocol and provision of a single step technique for biosynthetic processes, the use of biomaterials as the production assembly of silver nanoparticles has attracted interest [12].

The resinous material obtained by honeybees from different plant sources is known as propolis (bee glue). It is produced by bees through mixing collected tree buds with bee saliva, pollen, and wax [13,14]. The name propolis originated from the Greek words “pro” means “at the entry to” and “polis” means “place”, so the whole word “propolis” refers to a substance that protects the hive. Early beekeepers have known that propolis comes from a plant. Propolis' chemical diversity is determined by its plant origin. The chemical composition of bee glue is determined by the uniqueness of the local flora at the collection site, as well as the geographic and climatic characteristics of that location. More than 300 compounds have been found in propolis [15–17]. Resins (50 %), bee wax (30%), aromatic and essential oils (10 %), bee pollen (5%), and various organic compounds such as polyphenols, flavonoids, amino acids, vitamins, some alkaline earth materials, transition elements and micronutrients make up the majority of Propolis [18–20].

Egyptian propolis, according to the findings, has a complex chemical composition with just a few groups of chemicals identified. Phenolics seemed to be the primary constituents of Egyptian propolis (phenolic acids, their esters and flavonoids),

Scheme 1.

However, the quantities of phenolic acids in Egyptian propolis were lower than those of their esters, as found in European samples.



Populus nigra is thought to be one of the most plant sources of Egyptian propolis in Egypt. The presence of pentenyl caffeates and characteristic flavanones, as well as significant quantities of phenolic acid esters is due that [21]. The antimicrobial activity of propolis collected from four governorates in Upper Egypt was investigated against *Staphylococcus aureus*, *Escherichia coli*, and *Candida albicans*, and it was discovered that all propolis samples inhibited the growth of all bacteria tested, though the amount of inhibition varied depending on the propolis area [22]. In New Zealand and Egyptian propolis, caffeic acid phenethyl ester (CAPE) is a major bioactive component. CAPE has anticancer, anti-inflammatory, antioxidant, and other pharmacological properties [23,24]. Amira and Hiroshi also conducted a study on Propolis, which revealed that using bee products as an alternative therapy for COVID-19 may have positive outcomes [25].

The present research work aims to biosynthesis of AgNPs and study its applications as antibacterial agents. Moreover, we take advantage of the distinctive characteristics of the Egyptian propolis, which differs from the rest of the propolis over the world by virtue of the geographical location and the feed of the bees. In addition to combining the extract of this Egyptian propolis in an optimal way with silver precursor (AgNO_3), it was obtained the antimicrobial activity of AgNPs.

Experimental aspect:

2.1. Materials:

Commercial propolis belongs to Alwahaat area-Egypt was collected from the market. Silver nitrate (AgNO_3), sodium hydroxide (NaOH) and sulfuric acid (H_2SO_4) were purchased from Sigma Aldrich Chemicals. The Deionized water (DIW), ethanol, and HCl were all of analytical grade.

2.2 Characterization:

A Shimadzu Ultraviolet Spectrometer 2700 was used to record the absorption spectra to monitor and achieve the optimal synthesis of silver nanoparticles. To classify the potential biomolecules responsible for the reduction of Ag nanoparticles and capping of the bio-reduced nanoparticles, FT-IR analysis was performed at room temperature using a Nicolet 6700 FTIR spectrometer.

To study the thermal stability of biosynthesized Ag nanoparticles, thermo-gravimetric analyses were performed from 33 to 800°C with a heating rate of $10^\circ\text{C}/\text{min}$ using a LabSys EVO Setaram 1600 thermal analyzer. X-ray diffraction analysis of Ag nanoparticle crystalline growth was performed using a Bruker D8 Discover diffractometer equipped with a Cu microfocus X-ray source (1.5406nm) and a 2-dimensional Vantec 500 detector. On a glass slide, a drop of the nanoparticle suspension was deposited and dried. The measurements were taken with a step scan of 0.0052 in a 2-theta range of 5° to 80° . The data analysis was performed using the program Diffrac.Eva (Bruker).

To investigate the stability of the biosynthesized AgNPs and the degree of electrostatic or charge repulsion/attraction between the AgNPs, Zeta potential was measured using Nicomp 380 DLS/ZLS apparatus.

TEM analysis was carried out using a JEOL GEM-1010 transmission electron microscope with a 70 kV accelerating voltage to identify the particle size and the shape of AgNPs. A drop of a solution containing the particles was deposited on a copper grid and dried by allowing water to evaporate at room temperature.

To obtain qualitative information of elements in silver nanoparticles, EDX (FEI Quanta FEG 450) was used, which is one of the most practical, rapid, and suitable analytical methods for multi-element determination. As well as, nanostructure and morphology images of AgNPs were taken using

scanning electron microscopy SEM (FEI Quanta FEG 450) system.

2.3 Preparation of propolis extract:

In order to obtain an extract from Egyptian propolis, 0.5 g of propolis powder was added to 100 ml deionized water. The mixture was heated and stirred at 60°C for 30 min using hot plate with magnetic stirrer. Then the extract was cooled to room temperature and filtered with Whitman paper No.1 and stored at 4°C for further use.

2.4 Silver nanoparticles preparation:

An aqueous silver nitrate solution (10^{-3} M) was prepared by dissolving 0.017g of silver nitrate in 100 ml of deionized water. The biosynthesis of silver nanoparticles using propolis extract were carried out at different conditions such as the extract concentrations, the pH of the reaction solution and the reaction temperature to get the optimal conditions. To study the effect of Propolis extract quantity, a certain volume of the propolis extract (0.1 ml to 2 ml) was added to 1mL of AgNO_3 (10^{-3} M) solution and the volume was adjusted to 10 ml with de-ionized water. The final concentration of Ag^+ was 10^{-4} M. The reduction process of Ag^+ to Ag^0 nanoparticles was followed by the change in the color of the solution depending on the extract concentration.

To demonstrate the effect of pH, the mixture of 1mL of AgNO_3 and optimum volume the aqueous propolis extract was completed to 10mL with deionized water, and the pH was adjusted to pH (3,4,5,7,8 and 9) using NaOH and H_2SO_4 .

To study the effect of temperature, the mixture of 1ml of AgNO_3 aqueous solution with the optimum volume of propolis extract and DI water at the optimum pH value was prepared at different temperatures (25, 35, 45, 55, 65, 75 and 85°C).

To determine the optimum reaction time, two samples were prepared. The first sample was prepared by mixing an optimum volume of propolis extract and aqueous solution of silver nitrate at normal pH value, and the second sample was prepared with the optimum values of extract quantity, pH, and temperature. The reaction time was examined for the biosynthesis of silver nanoparticles over a period of time of 70 minutes. The formation of silver nanoparticles, in all above experiments, was monitored using UV-Vis spectrophotometer.

2.5 Anti-microbial experiment design:

The antimicrobial activities of the samples tested were studied on Mueller–Hinton agar plates by Agar diffusion technique against Gram-positive (*S. aureus*) and Gram-negative (*E. coli*) bacterial strain. Nitrofurantoin (300 µg/ml) was used as the standard antibacterial agent. The antimicrobial effect of Ag-NPs was tested at concentration of 0.5mg/ml and as optimal prepared sample. Mueller–Hinton agar plates seeded with 1.8×10^8 cfu/mL (0.5 OD^{600}) of the test bacteria. Following 24 hrs incubation at 37 °C, plates were examined for the presence of inhibition zones. The inhibition zones surrounding the wells were measured (mm) considering only halos >6 mm. Inhibition zones obtained are the mean of three replicates for each experiment [26].

3. Results and Discussion

3.1-UV-Visible spectrophotometer results:

UV–Visible spectra of the prepared nanoparticles were recorded to determine the surface Plasmon resonance (SPR), band of the AgNPs. From the position, width, and shape of the SPR band a qualitative idea concerning the shape and size of nanoparticles can be obtained. The color of the solutions changed from light yellow to yellowish-brown to deep brown as the extract content rises, implying silver nanoparticle formation as the surface Plasmon resonance (SPR) of AgNPs is 420–458 nm [27].

3.2.1 Effect of propolis extract quantity:

The absorption spectra of the extract and biosynthesized silver nanoparticles were recorded against deionized water. The absorption spectrum of the 1 ml extract showed a maximum at 276 nm and shoulder at 366 nm due π – π^* and ν – π^* transitions, respectively.

Figure 1, shows the UV–visible spectra show the synthesis of silver nanoparticles at a constant AgNO_3 concentration (1×10^{-3} M) with different quantities of the extract. The increasing of extract concentration from 0.1ml to 2ml causes an increase in the formation of AgNPs. The peak of absorbance was blue shifted from 438nm to 426 nm. This means that the AgNPs mean diameter has slightly decreased in particle size. These results are in agreement with previous reports of biosynthesis of silver nanoparticles [28, 29].

3.1.2 Effect of pH:

The effect of pH on the formation of silver nanoparticles is shown in Figure 2. At pH 3, there was no SPR peak observed, while a clear SPR peak characteristic for the AgNPs started from pH 4. As

the pH was further increased from 4 to 8, the SPR peak rises and become somewhat sharper and slightly shifted and then falls at pH 9 or higher. Moreover, at higher pH conditions, all absorbance spectra depicted a single sharper peak around 434 nm, illustrating the formation of regular spherically shaped AgNPs [30] which was further confirmed by TEM studies. Furthermore, the brown color of the nanoparticles was observed shortly after the AgNO_3 was mixed with the extract. These observations manifest the efficient reduction of silver ions in the presence of hydroxide ions (OH^-) due to increased pH. Prior research has shown that changing the pH of reaction mixtures can affect the size and shape of biosynthesized nanoparticles. The capacity of the reaction pH to alter the electrical charges of biomolecules, which may affect their capping and stabilizing abilities and, as a result, the growth of nanoparticles, is a significant influence. The formation of silver nanoparticles in the basic medium is predicted to be greater than in the acidic medium [31]. In comparison to other pH values, the absorbance curve became more narrow and reached a maximum value at pH= 8. This leads to the conclusion that the size of nanoparticles is decreased, which may be due to decreasing particle aggregation due to full charging of the clusters, which maximized repulsive electrostatic interactions [32].

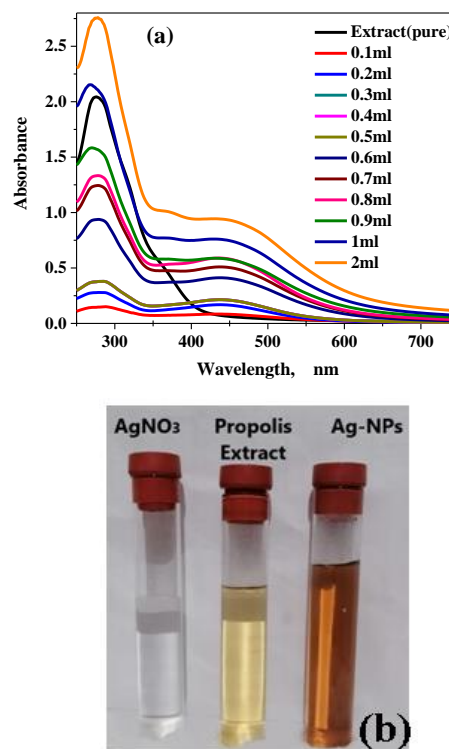


Figure 1: a) Effect of propolis extract quantity on biosynthesis of AgNPs; b) The photo of biosynthesized AgNPs.

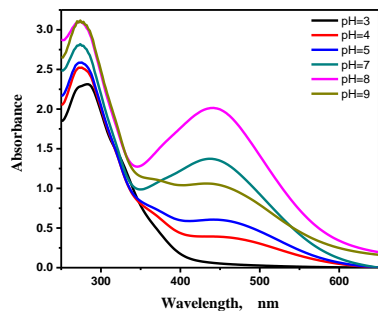


Figure 2: The effect of pH on biosynthesis of silver nanoparticles.

3.1.3 Temperature effect:

The UV-visible spectra of silver nanoparticles prepared at various temperatures are shown in Figure 3. It can be shown that as the temperature rises, the absorbance rises as well. This experiment suggests that increasing the temperature of the reaction mixture will speed up the slow rate of AgNPs at ambient temperature. The formation of small AgNPs was allowed by increasing the reaction temperature, which resulted in an accelerated reduction rate of Ag⁺ ions and subsequent homogeneous nucleation of silver nuclei. The results in Figure 3 show that the efficiency of silver nanoparticles synthesis was highest at 75 °C. Further increase did not change the absorption maximum, while there is small blue shift indicating smaller nanoparticles size is predictable [27,33].

It is noted that the maximum absorbance at room temperature was at 428 nm and almost no change in the spectra in the extract region. However, this range is disturbed by changing solution pH and temperature during synthesis. The effect of increasing the pH to 8 and temperature to 75 °C is reflected on the time of reaction which decreased to 11 min at optimum pH and temperature.

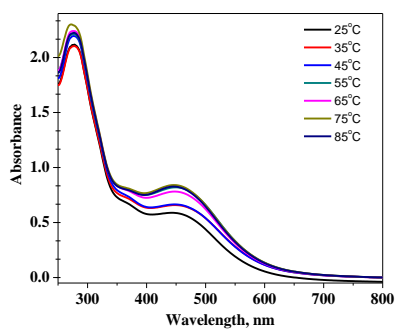


Figure 3: The effect of temperature on biosynthesis of silver nanoparticles.

3.1.4 The Reaction Time

The energy of heating is well known for speeding up the reaction of a mixture. This was demonstrated in these studies, as shown in Figure 5. The reaction between Ag⁺ and the reducing material in propolis extract was studied. Figure 5(a)&(b) display the UV-visible spectra of silver nanoparticles as a function of time after adding 2 ml of propolis extract into 1 ml AgNO₃. The absorbance range with SPR at 444 nm gradually increased as the reaction time was increased, and the color intensity increased with the duration of incubation. As the reaction time went on, the amplitude of the SPR peak increased, indicating higher silver nanoparticle concentrations. This means that the silver nanoparticles made using this green synthesis process are very stable and do not agglomerate. The time of incubation was estimated at room temperature and 75 °C. It is observed that the maximum absorbance at 75 °C was in 11min [33, 34] and one hour at room temperature.

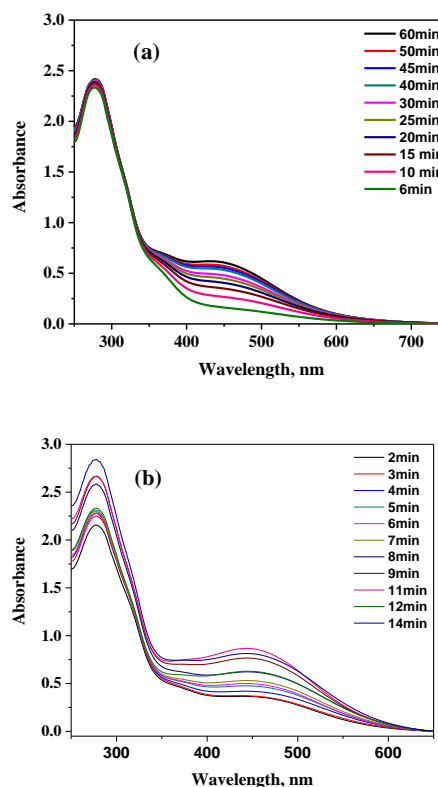


Figure-5: The reaction time of biosynthesis silver nanoparticles at room temperature (a) and at optimum condition (pH=8 and 65 °C) (b)

3.2 XRD analysis

One of the utmost significant evidence for the creation of Ag nanoparticles is the X-ray diffraction patterns. As these AgNPs combine with each other during crystallization to form a cube-system crystal.

Figure 6 depicts the X-ray diffraction patterns of dried Ag nanoparticles synthesized at 35 °C using propolis extract and at pH 8. The XRD results of Ag/extract revealed that silver nanoparticles have a face-centered cubic (fcc) structure. The 111, 200, 220, 311, and 222 crystallographic planes are also to be attributed to the XRD peaks at 2θ of 38°, 46.16°, 64.98°, and 77.56°. These planes and angles of XRD of Ag-NPs were compared with diffraction card PXRD Reference Number 00–029–1493. The effect of the extract is shown in broadening the background of XRD patterns. The peaks at different positions, which is due to bioorganic compounds presented in the extract and some impurities due to the presence of traces of transition metal ions in the aqueous propolis extract [27, 35, 36].

As can be seen from the XRD pattern, Ag-NPs made with propolis extract were basically crystalline. The average nanocrystalline size was calculated using the well-known Debye–Scherrer formula, $D = \lambda k / \beta \cos \theta$, where D is the crystal size, k is a constant and equals unity, λ is the X-ray source wavelength (0.1541 nm), β is the full width at half maximum (FWHM), and θ is the diffraction angle corresponding to the lattice plane (111) [37].

The average crystallite dimension, measured using the Debye–Scherrer equation, is 9.43 nm. Whereas the average nanocrystalline over the lattice planes of AgNPs is 13.09 nm. From these data, it is noted the agreement between XRD results and TEM results regarding particle size

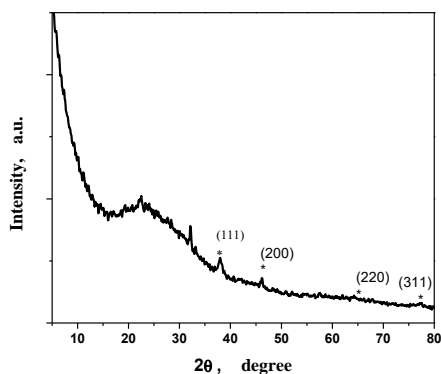


Figure 6 XRD patterns of biosynthesized AgNPs at 35 °C, pH 8.

3.3 FT-IR analysis

For the AgNPs and propolis extract, the FTIR analysis showed many distinct bands (Figure 7).

The FTIR spectrum showed band at 3369 cm^{-1} corresponds to hydroxyl groups (O–H), was attributed to the presence of flavonoid and phenolic compounds in the propolis extract [38]. The bands at 2927 cm^{-1} and 2851 cm^{-1} were corresponded to the symmetrical stretches of CH_3 and asymmetrical stretches of CH_2 , respectively, suggesting the existence of long-chain alkyl compounds in the propolis extract [39]. These absorptions bands were correlated or associated - with waxes residues of the extract [40]. The absorptions bands at 1701 cm^{-1} (C=O), 1614 cm^{-1} (C=C), 1454 cm^{-1} (aromatic C–H) and at 1365 cm^{-1} (aromatic C–O), were associated with the presence of flavonoids. The profile of infrared spectrum obtained for the propolis extract studied, was very similar to the previous data published for propolis from other origins [41,42]. By comparing these two spectra, it is noted that the phenolic hydroxyl groups (O–H), which is predicted to be responsible for bio-reduction of silver nitrate, was shifted from 3369 cm^{-1} (propolis extract) to 3357 cm^{-1} (AgNPs) [43,44]. While there is no shift in C=C groups could be detected, the aromatic C–O exhibit a considerable shift from 1365 to 1388 cm^{-1} .

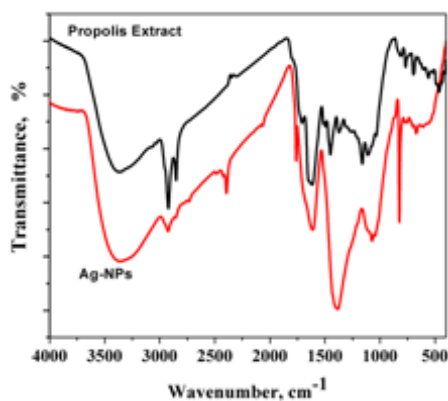


Figure 7 FT-IR spectra of propolis extract and capped AgNPs.

3.4 Thermogravimetric analyses:

In figure 8, the biomolecules that capped the surface of Ag nanoparticles was further illustrated with TGA analysis. There are two forms of weight loss with rising temperature, according to the thermogravimetric analysis curve. The first is sudden weight loss over a small temperature range (37 %

weight loss) ranging from 87 to 162 °C. The adsorbed water molecules and possibly the flavonoid groups that envelop the silver nanoparticles are responsible for the weight loss at these temperatures. The flavonoids group decomposes in the range of temperature between 50 to 150 °C [45].

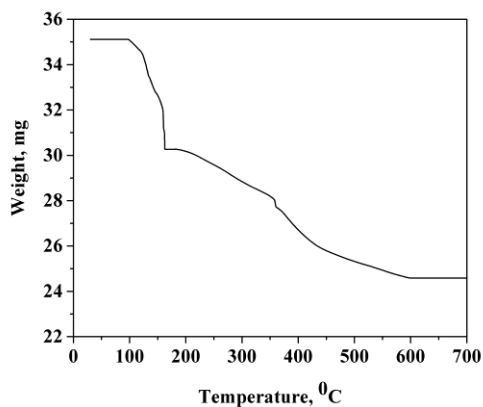


Figure 8 The TGA analysis of biosynthesized AgNPs.

The second step is a steady and gradual loss of sample weight that begins at 220 °C and ends at 624 °C. The organic compounds in the extract degrade during this period, including phenolic group (in the range of 150 to 350°C) [46], which is also one of the materials that capping nanoparticles. This second type of weight loss accounts for 17% of the total sample weight.

3.5 Zeta potential

The zeta potential is the charge at a short distance from the surface of the particle. Zeta potential is analyzed by applying an electric field to the suspension and measuring the speed and direction of the particle motion. The primary result from a zeta potential measurement is the electrophoretic mobility μ which is then used to calculate the zeta potential using the equation:

$$\xi = \eta\mu/\varepsilon$$

Where, ξ is zeta potential, η is the viscosity of the AgNPs solvent, μ is the electrophoretic mobility, and ε is the dielectric constant of the AgNPs solvent [47].

To evaluate the average size, size distribution, and possible aggregation, zeta potential, of AgNPs, a simplified optical diagram of the Nicomp system is used. Figure-9 is the zeta potential of biosynthesized silver nanoparticles.

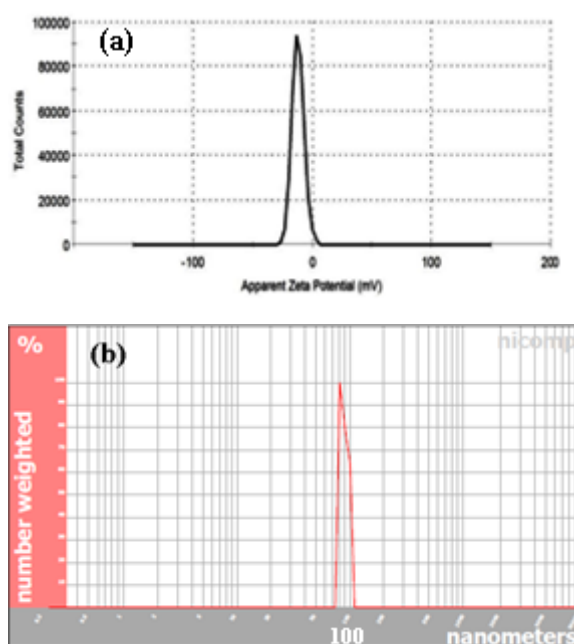


Figure 9 Zeta potential (a) and the size distribution by number (b) of biosynthesized AgNPs.

The size distribution results show that the particles size using this method or Z-average of ~ 100 nm was so large and this value is larger than that measured by TEM or XRD. This is due that DLS gives the hydrodynamic radius while TEM gives the actual size. As well, DLS measures the size distribution that differentiates from TEM, i.e., it increasing mistake of measuring the large particles due to their much stronger scattered light intensity. So, the size obtained from TEM will be the actual size of silver nanoparticles [48]. The increase of the dynamic size may be due to the increase of the bio-organic from the extract on the surface of the AgNPs.

The zeta potential of biosynthesized AgNPs was determined, and the results indicate that the nanoparticles' surfaces are negatively charged (-8.8 mV) and well distributed in the medium. The particles with zeta potential values between +30 and -30 mV are considered to be in a stable suspension [49].

3.6 SEM and EDX measurements:

A scanning electron microscope (SEM) was used to examine the morphology of silver nanoparticles made with propolis extract (Figure 9). The product consists primarily of non-uniform shapes of sphere-like shapes, as shown in a typical SEM picture. These shapes were crammed in close proximity to one another. Moreover, closer examination with a high resolution showed that the size of silver nanoparticles is between 8.3 and 40.1 nm.

The chemical composition of biosynthesized silver nanoparticles using the propolis extract was obtained using energy-dispersive X-ray spectroscopy (EDX) (Figure 10). Silver's strong signal was obtained at energy of 3.87 keV, as well as some of the weak signals from Na, Cl, K, O, Mg, and Al, were obtained at energy of 0.43 keV. The elemental weights in the nanoparticles show that silver has the highest value (67.85%) and can be classified correctly.

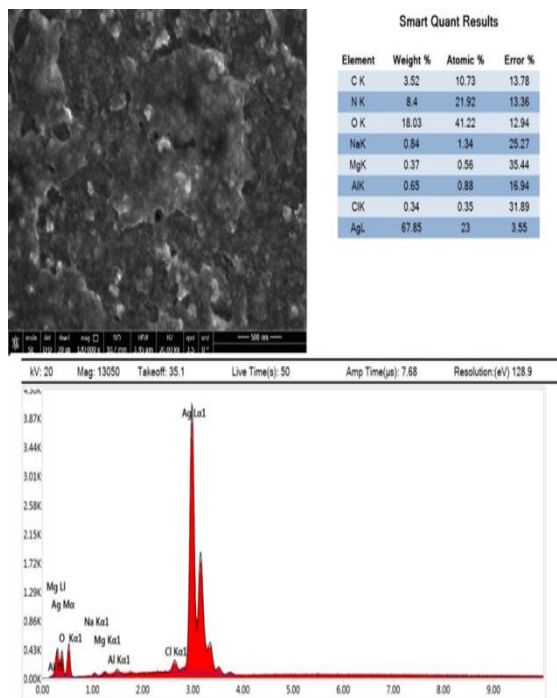


Figure 10 SEM and EDAX data of biosynthesized AgNPs

3.7 TEM measurements:

In Figure 11, a representative TEM image of silver nanoparticles synthesized by Egyptian propolis is shown. The silver nanoparticles are relatively uniform in diameter and spherical in shape, according to the TEM picture. The particles' average size was determined to be 11.39 nm and this value agreed with the reported value for silver nanoparticles synthesized using propolis, previously [50,51] and in agreement with the size obtained from XRD calculations of the AgNPs that ranged between 9.43 nm to 13.09nm.

It was observed that the particle size measured from TEM measurements is smaller than that obtained from dynamic light scattering measurements. This is because the particle size, in dynamic light scattering measurements, is greatly increased by contributions from capping agents as well as solvation effects.

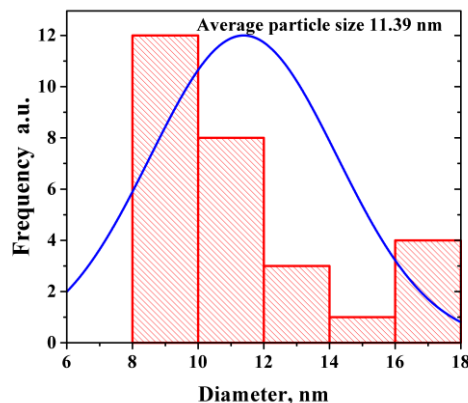
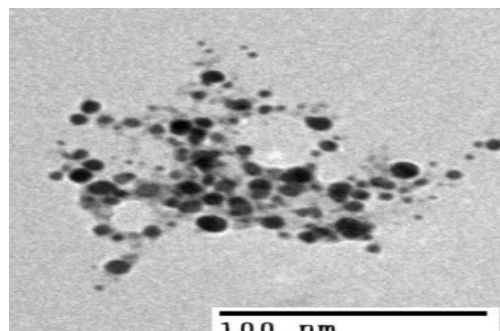


Figure 11 TEM image of biosynthesized AgNPs.

3.8 Anti-microbial activity of AgNPs:

The antimicrobial efficiency of propolis varies greatly depending on the extraction procedure of the crude material and the solvents used in this process. Juga found that the highest extraction efficiency of flavones and flavonols (21% w/v) was obtained when 80% ethanol while water appeared to be the least efficient extraction medium, resulting in extracts containing only around 0.6%, w/v, of flavones and flavonols. This is attributed to the rather poor aqueous solubility of those compounds. Previous studies for antimicrobial activity of the propolis aqueous extract used higher concentrations of the extract (10g/20 ml at 60 °C for 7 h) [52][53].

All of silver ions, AgNPs, and propolis have long been known to have potent antimicrobial properties [16,54]. The antibacterial activity of AgNPs against *S. aureus* and *E.coli* using AgNPs as prepared and dried nanoparticles as well as the extract is shown in Table 1. Silver nanoparticles have no effect on *S. aureus*. AgNPs have the highest antimicrobial activity against *Escherichia coli*, according to the findings. As compared to the previous study [55], this value indicates that biosynthesized Silver nanoparticles with Egyptian propolis gave more antimicrobial activity against these *E.coli* [56, 57]. Because the

propolis extract was in such a low concentration (0.5g/100ml), it had no effect on bacteria.

The main role of silver nanoparticles' antibacterial activity on microbes has yet to be identified, but it could be related to the mechanism of Ag⁺ ions action toward bacteria or microbes, in which the accumulation of silver NPs from the aqueous solution saturates the cell's enzymes and proteins gradually. It has been suggested that silver nanoparticles have three antibacterial mechanisms. The first mechanism is the adhesion of nanoparticles to the cell wall, which prevents the growth and reproduction of bacteria, and this leads to disruption of the function of the cell wall in protecting the inner part of the cell. Second mechanism, modifying the normal development of nucleic acid, silver nanoparticles enters into the bacterial cell, causing cell death or at least DNA damage. Third mechanism, the bacterial cell wall is irreversibly disrupted by the engagement of Ag⁺ ions with sulfur-containing proteins in the cell wall. When testing antimicrobial activity, this proposed mechanism was also concluded as the primary antibacterial mechanism [58–61].

Silver nanoparticles antimicrobial activity is influenced by various factors, including particle size, shape, surface charge, and morphology. Because of the structure of the bacterial cell wall, nanoparticles can penetrate into the nuclear content of bacteria, inactivating DNA and enzymes and causing cellular death, particularly in gram-negative bacteria [62,63].



Figure 11 Antimicrobial activity tests of biosynthesized AgNPs and propolis extract.

Table 1: Inhibitory effect of biosynthesized silver nanoparticles using Egyptian propolis on different Germs (Inhibition Zones as mm).

| Sample | Pathogenic microorganism | |
|-------------------------|---|--|
| | <i>Staphylococcus aureus</i> Gram (+ve) bacteria | <i>Escherichia coli</i> Gram (-ve) bacteria |
| Nitrofurantoin(control) | 15 | 18 |
| Propolis extract | NA | NA |
| Ag-NPs solid sample | NA | 22 |
| Ag-NPs as prepared | NA | 18 |

Conclusion

The facile and green method of bio-reduction of aqueous AgNO₃ by the aqueous extract of the Egyptian propolis was demonstrated and Ag-NPs were produced with average size ranging from 9.43nm to 13.09nm. The biosynthesis of silver nanoparticles showed that the preparation process was easy to control in terms of the speed of reduction within 13 minutes, moderate pH and temperature of 75 °C. The use of propolis in the green synthesis of silver nanoparticles opens the door to a plethora of new bio-nanotechnology applications. For example, bio-reduced AgNPs may be used as an active ingredient to treat a variety of human diseases.

Conflicts of interest

All authors declare that they have no conflict of interest.

References

- [1] Shukla, A. K.; Iravani, S. Green Synthesis, Characterization and Applications of Nanoparticles; Elsevier, 2018.
- [2] Parveen, K.; Banse, V.; Ledwani, L. Green Synthesis of Nanoparticles: Their Advantages and Disadvantages. In AIP conference proceedings; AIP Publishing LLC, 2016; Vol. 1724, p 20048.
- [3] Zhu, X.; Pathakoti, K.; Hwang, H.-M. Green Synthesis of Titanium Dioxide and Zinc Oxide Nanoparticles and Their Usage for Antimicrobial Applications and Environmental Remediation. In Green Synthesis, Characterization and Applications of Nanoparticles; Elsevier, 2019; pp 223–263.
- [4] Beyene, H. D.; Werkneh, A. A.; Bezabh, H. K.; Ambaye, T. G. Synthesis Paradigm and Applications of Silver Nanoparticles (AgNPs), a Review. *Sustain. Mater. Technol.*, 2017, 13, 18–23.

- [5] Vijayakumar, S.; Divya, M.; Vaseeharan, B.; Chen, J.; Biruntha, M.; Silva, L. P.; Duran-Lara, E. F.; Shreema, K.; Ranjan, S.; Dasgupta, N. Biological Compound Capping of Silver Nanoparticle with the Seed Extracts of Blackcumin (*Nigella Sativa*): A Potential Antibacterial, Antidiabetic, Anti-Inflammatory, and Antioxidant. *J. Inorg. Organomet. Polym. Mater.*, 2021, 31 (2), 624–635.
- [6] Bhardwaj, D.; Singh, R. Green Biomimetic Synthesis of Ag–TiO₂ Nanocomposite Using *Origanum Majorana* Leaf Extract under Sonication and Their Biological Activities. *Bioresour. Bioprocess.*, 2021, 8 (1), 1–12.
- [7] Husen, A.; Siddiqi, K. S. Phytosynthesis of Nanoparticles: Concept, Controversy and Application. *Nanoscale Res. Lett.*, 2014, 9 (1), 1–24.
- [8] Sajadi, S. M.; Nasrollahzadeh, M.; Maham, M. Aqueous Extract from Seeds of *Silybum Marianum* L. as a Green Material for Preparation of the Cu/Fe₃O₄ Nanoparticles: A Magnetically Recoverable and Reusable Catalyst for the Reduction of Nitroarenes. *J. Colloid Interface Sci.*, 2016, 469, 93–98.
- [9] Nam, G.; Purushothaman, B.; Rangasamy, S.; Song, J. M. Investigating the Versatility of Multifunctional Silver Nanoparticles: Preparation and Inspection of Their Potential as Wound Treatment Agents. *Int. Nano Lett.*, 2016, 6 (1), 51–63.
- [10] Firdhouse, M. J.; Lalitha, P. Biosynthesis of Silver Nanoparticles and Its Applications. *J. Nanotechnol.*, 2015, 2015.
- [11] Sharma, V. K.; Yngard, R. A.; Lin, Y. Silver Nanoparticles: Green Synthesis and Their Antimicrobial Activities. *Adv. Colloid Interface Sci.*, 2009, 145 (1–2), 83–96.
- [12] Ahmed, S.; Ahmad, M.; Swami, B. L.; Ikram, S. A Review on Plants Extract Mediated Synthesis of Silver Nanoparticles for Antimicrobial Applications: A Green Expertise. *J. Adv. Res.*, 2016, 7 (1), 17–28.
- [13] Ali, A. M.; Kunugi, H. Apitherapy for Age-Related Skeletal Muscle Dysfunction (Sarcopenia): A Review on the Effects of Royal Jelly, Propolis, and Bee Pollen. *Foods*, 2020, 9 (10), 1362.
- [14] Ali, A. M.; Kunugi, H. Apitherapy for Parkinson's Disease: A Focus on the Effects of Propolis and Royal Jelly. *Oxid. Med. Cell. Longev.*, 2020, 2020.
- [15] Anjum, S. I.; Ullah, A.; Khan, K. A.; Attaullah, M.; Khan, H.; Ali, H.; Bashir, M. A.; Tahir, M.; Ansari, M. J.; Ghramh, H. A. Composition and Functional Properties of Propolis (Bee Glue): A Review. *Saudi J. Biol. Sci.*, 2019, 26 (7), 1695–1703.
- [16] Kocot, J.; Kielczykowska, M.; Luchowska-Kocot, D.; Kurzepa, J.; Musik, I. Antioxidant Potential of Propolis, Bee Pollen, and Royal Jelly: Possible Medical Application. *Oxid. Med. Cell. Longev.*, 2018, 2018.
- [17] Hashem, H. IN Silico Approach of Some Selected Honey Constituents as SARS-CoV-2 Main Protease (COVID-19) Inhibitors. *Eurasian J. Med. Oncol*, 2020, 4, 196–200.
- [18] Ghisalberti, E. L. Propolis: A Review. *Bee world*, 1979, 60 (2), 59–84.
- [19] Bankova, V. Recent Trends and Important Developments in Propolis Research. Evidence-based Complement. *Altern. Med.*, 2005, 2 (1), 29–32.
- [20] Castaldo, S.; Capasso, F. Propolis, an Old Remedy Used in Modern Medicine. *Fitoterapia*, 2002, 73, S1–S6.
- [21] Christov, R.; Bankova, V.; Hegazi, A.; Abd El Hady, F.; Popov, S. Chemical Composition of Egyptian Propolis. *Zeitschrift für Naturforsch. C*, 1998, 53 (3–4), 197–200.
- [22] Hegazi, A. G.; Abd El Hady, F. K. Egyptian Propolis: 1-Antimicrobial Activity and Chemical Composition of Upper Egypt Propolis. *Zeitschrift für Naturforsch. C*, 2001, 56 (1–2), 82–88.
- [23] Refaat, H.; Mady, F. M.; Sarhan, H. A.; Rateb, H. S.; Alaaeldin, E. Optimization and Evaluation of Propolis Liposomes as a Promising Therapeutic Approach for COVID-19. *Int. J. Pharm.*, 2021, 592, 120028.
- [24] Bhargava, P.; Grover, A.; Nigam, N.; Kaul, A.; Ishida, Y.; Kakuta, H.; Kaul, S. C.; Terao, K.; Wadhwa, R. Anticancer Activity of the Supercritical Extract of Brazilian Green Propolis and Its Active Component, Artepillin C: Bioinformatics and Experimental Analyses of Its Mechanisms of Action. *Int. J. Oncol.*, 2018, 52 (3), 925–932.
- [25] Ali, A. M.; Kunugi, H. Propolis, Bee Honey, and Their Components Protect against Coronavirus Disease 2019 (Covid-19): A Review of in Silico, in Vitro, and Clinical Studies. *Molecules*, 2021, 26 (5), 1232.
- [26] Wikler, M. A. Methods for Dilution Antimicrobial Susceptibility Tests for Bacteria That Grow Aerobically: Approved Standard. CLSI, 2006, 26, M7-A7.
- [27] Khalil, M. M. H.; Ismail, E. H.; El-Baghdady, K. Z.; Mohamed, D. Green Synthesis of Silver Nanoparticles Using Olive Leaf Extract and Its Antibacterial Activity. *Arab. J. Chem.*, 2014, 7 (6), 1131–1139.
- [28] Mishra, Y. K.; Mohapatra, S.; Kabiraj, D.; Mohanta, B.; Lalla, N. P.; Pivin, J. C.; Avasthi, D. K. Synthesis and Characterization of Ag Nanoparticles in Silica Matrix by Atom Beam Sputtering. *Scr. Mater.*, 2007, 56 (7), 629–632.
- [29] Anigol, L. B.; Charantimath, J. S.; Gurubasavaraj, P. M. Effect of Concentration and Ph on the Size of Silver Nanoparticles Synthesized by Green Chemistry. *Org. Med. Chem. Int. J*, 2017, 3, 1–5.
- [30] Ismail, E. H.; Khalil, M. M. H.; Al Seif, F. A.; El-Magdoub, F.; Bent, A. N.; Rahman, A.; Al, U. S. D. Biosynthesis of Gold Nanoparticles Using Extract of Grape (*Vitis Vinifera*) Leaves and Seeds. *Prog Nanotechnol Nanomater*, 2014, 3, 1–12.
- [31] Konwarh, R.; Gogoi, B.; Philip, R.; Laskar, M. A.; Karak, N. Biomimetic Preparation of Polymer-Supported Free Radical Scavenging, Cytocompatible and Antimicrobial “Green” Silver Nanoparticles Using Aqueous Extract of *Citrus Sinensis* Peel. *Colloids Surfaces B Biointerfaces*, 2011, 84 (2), 338–345.

- [32] Wisam, J. A.; Haneen, A. J. A Novel Study of PH Influence on Ag Nanoparticles Size with Antibacterial and Antifungal Activity Using Green Synthesis. *World Sci. News*, 2018, 97, 139–152.
- [33] Kasture, M. B.; Patel, P.; Prabhune, A. A.; Ramana, C. V.; Kulkarni, A. A.; Prasad, B. L. V. Synthesis of Silver Nanoparticles by Sophorolipids: Effect of Temperature and Sophorolipid Structure on the Size of Particles. *J. Chem. Sci.*, 2008, 120 (6), 515–520.
- [34] Chen, D.; Qiao, X.; Qiu, X.; Chen, J. Synthesis and Electrical Properties of Uniform Silver Nanoparticles for Electronic Applications. *J. Mater. Sci.*, 2009, 44 (4), 1076–1081.
- [35] Okaiyeto, K.; Hoppe, H.; Okoh, A. I. Plant-Based Synthesis of Silver Nanoparticles Using Aqueous Leaf Extract of *Salvia officinalis*: Characterization and Its Antiplasmodial Activity. *J. Clust. Sci.*, 2021, 32 (1), 101–109.
- [36] Acharya, D.; Satapathy, S.; Somu, P.; Parida, U. K.; Mishra, G. Apoptotic Effect and Anticancer Activity of Biosynthesized Silver Nanoparticles from Marine Algae *Chaetomorpha Linum* Extract against Human Colon Cancer Cell HCT-116. *Biol. Trace Elem. Res.*, 2021, 199 (5), 1812–1822.
- [37] Scherrer, P. *Nachr Ges Wiss Goettingen. Math. Phys.*, 1918, 2, 98–100.
- [38] Do Nascimento, T. G.; Da Silva, P. F.; Azevedo, L. F.; Da Rocha, L. G.; de Moraes Porto, I. C. C.; e Moura, T. F. A. L.; Basílio-Júnior, I. D.; Grillo, L. A. M.; Dornelas, C. B.; da Silva Fonseca, E. J. Polymeric Nanoparticles of Brazilian Red Propolis Extract: Preparation, Characterization, Antioxidant and Leishmanicidal Activity. *Nanoscale Res. Lett.*, 2016, 11 (1), 1–16.
- [39] Woźniak, M.; Kwaśniewska-Sip, P.; Krueger, M.; Roszyk, E.; Ratajczak, I. Chemical, Biological and Mechanical Characterization of Wood Treated with Propolis Extract and Silicon Compounds. *Forests*, 2020, 11 (9), 907.
- [40] Ramli, N. A.; Ali, N.; Hamzah, S.; Yatim, N. I. Physicochemical Characteristics of Liposome Encapsulation of Stingless Bees' Propolis. *Heliyon*, 2021, 7 (4), e06649.
- [41] Oliveira, R. N.; Mancini, M. C.; Oliveira, F. C. S. de; Passos, T. M.; Quilty, B.; Thiré, R. M. da S. M.; McGuinness, G. B. FTIR Analysis and Quantification of Phenols and Flavonoids of Five Commercially Available Plants Extracts Used in Wound Healing. *Matéria (Rio Janeiro)*, 2016, 21, 767–779.
- [42] Hussein, U. K.; Hassan, N. E.-H. Y.; Elhalwagy, M. E. A.; Zaki, A. R.; Abubakr, H. O.; Nagulapalli Venkata, K. C.; Jang, K. Y.; Bishayee, A. Ginger and Propolis Exert Neuroprotective Effects against Monosodium Glutamate-Induced Neurotoxicity in Rats. *Molecules*, 2017, 22 (11), 1928.
- [43] Zargar, M.; Shameli, K.; Najafi, G. R.; Farahani, F. Plant Mediated Green Biosynthesis of Silver Nanoparticles Using *Vitex Negundo* L. Extract. *J. Ind. Eng. Chem.*, 2014, 20 (6), 4169–4175.
- [44] Abbas, O.; Compère, G.; Larondelle, Y.; Pompeu, D.; Rogez, H.; Baeten, V. Phenolic Compound Explorer: A Mid-Infrared Spectroscopy Database. *Vib. Spectrosc.*, 2017, 92, 111–118.
- [45] Chaaban, H.; Ioannou, I.; Chebil, L.; Slimane, M.; Gérardin, C.; Paris, C.; Charbonnel, C.; Chekir, L.; Ghoul, M. Effect of Heat Processing on Thermal Stability and Antioxidant Activity of Six Flavonoids. *J. Food Process. Preserv.*, 2017, 41 (5), e13203.
- [46] Cheng, Y.; Xu, Q.; Liu, J.; Zhao, C.; Xue, F.; Zhao, Y. Decomposition of Five Phenolic Compounds in High Temperature Water. *J. Braz. Chem. Soc.*, 2014, 25, 2102–2107.
- [47] Vanitha, G.; Rajavel, K.; Boopathy, G.; Veeravazhuthi, V.; Neelamegam, P. Physicochemical Charge Stabilization of Silver Nanoparticles and Its Antibacterial Applications. *Chem. Phys. Lett.*, 2017, 669, 71–79.
- [48] Bhattacharjee, S. DLS and Zeta Potential—What They Are and What They Are Not? *J. Control. Release*, 2016, 235, 337–351.
- [49] Tuan, T. Q.; Van Hao, P.; Quynh, L. M.; Luong, N. H.; Hai, N. H. Preparation and Properties of Silver Nanoparticles by Heat-Combined Electrochemical Method. *VNU J. Sci. Math.*, 2015, 31 (2).
- [50] Priyadarshini, J. F.; Sivakumari, K.; Selvaraj, R.; Ashok, K.; Jayaprakash, P.; Rajesh, S. Green Synthesis of Silver Nanoparticles from Propolis. *Res J Life Sci Bioinform Pharm Chem Sci*, 2018, 4, 23–36.
- [51] Barbosa, V. T.; Souza, J. K. C.; Alvino, V.; Meneghetti, M. R.; Florez-Rodriguez, P. P.; Moreira, R. E.; Paulino, G. V. B.; Landell, M. F.; Basílio-Júnior, I. D.; do Nascimento, T. G. Biogenic Synthesis of Silver Nanoparticles Using Brazilian Propolis. *Biotechnol. Prog.*, 2019, 35 (6), e2888.
- [52] Al-Ani, I.; Zimmermann, S.; Reichling, J.; Wink, M. Antimicrobial Activities of European Propolis Collected from Various Geographic Origins Alone and in Combination with Antibiotics. *Medicines*, 2018, 5 (1), 2.
- [53] Jug, M.; Karas, O.; Kosalec, I. The Influence of Extraction Parameters on Antimicrobial Activity of Propolis Extracts. *Nat. Prod. Commun.*, 2017, 12 (1), 1934578X1701200113.
- [54] Furno, F.; Morley, K. S.; Wong, B.; Sharp, B. L.; Arnold, P. L.; Howdle, S. M.; Bayston, R.; Brown, P. D.; Winship, P. D.; Reid, H. J. Silver Nanoparticles and Polymeric Medical Devices: A New Approach to Prevention of Infection? *J. Antimicrob. Chemother.*, 2004, 54 (6), 1019–1024.
- [55] Li, J.; Rong, K.; Zhao, H.; Li, F.; Lu, Z.; Chen, R. Highly Selective Antibacterial Activities of Silver Nanoparticles against *Bacillus Subtilis*. *J. Nanosci. Nanotechnol.*, 2013, 13 (10), 6806–6813.
- [56] Alsamhary, K. I. Eco-Friendly Synthesis of Silver Nanoparticles by *Bacillus Subtilis* and Their Antibacterial Activity. *Saudi J. Biol. Sci.*, 2020, 27 (8), 2185–2191.
- [57] Edis, Z.; Haj Bloukh, S.; Ibrahim, M. R.; Abu Sara, H. “Smart” Antimicrobial Nanocomplexes with Potential to Decrease

- Surgical Site Infections (SSI). *Pharmaceutics*, 2020, 12 (4), 361.
- [58] Li, Q.; Mahendra, S.; Lyon, D. Y.; Brunet, L.; Liga, M. V; Li, D.; Alvarez, P. J. J. Antimicrobial Nanomaterials for Water Disinfection and Microbial Control: Potential Applications and Implications. *Water Res.*, 2008, 42 (18), 4591–4602.
- [59] Pal, S.; Tak, Y. K.; Song, J. M. Does the Antibacterial Activity of Silver Nanoparticles Depend on the Shape of the Nanoparticle? A Study of the Gram-Negative Bacterium *Escherichia Coli*. *Appl. Environ. Microbiol.*, 2007, 73 (6), 1712–1720.
- [60] Morones, J. R.; Elechiguerra, J. L.; Camacho, A.; Holt, K.; Kouri, J. B.; Ramírez, J. T.; Yacaman, M. J. The Bactericidal Effect of Silver Nanoparticles. *Nanotechnology*, 2005, 16 (10), 2346.
- [61] Keat, C. L.; Aziz, A.; Eid, A. M.; Elmarzug, N. A. Biosynthesis of Nanoparticles and Silver Nanoparticles. *Bioresour. Bioprocess.*, 2015, 2 (1), 1–11.
- [62] Siddiqi, K. S.; Husen, A.; Rao, R. A. K. A Review on Biosynthesis of Silver Nanoparticles and Their Biocidal Properties. *J. Nanobiotechnology*, 2018, 16 (1), 1–28.
- [63] Gamboa, S. M.; Rojas, E. R.; Martínez, V. V.; Vega-Baudrit, J. Synthesis and Characterization of Silver Nanoparticles and Their Application as an Antibacterial Agent. *Int. J. Biosen. Bioelectron*, 2019, 5, 166–173.